Romanian Reports in Physics, Vol. 60, No. 3, P. 749–761, 2008

Dedicated to Prof. Ioan-Iovitz Popescu's 75th Anniversary

OPTICS AND QUANTUM ELECTRONICS

GINZBURG-LANDAU SPATIOTEMPORAL DISSIPATIVE OPTICAL SOLITONS

D. MIHALACHE, D. MAZILU

Horia Hulubei National Institute for Physics and Nuclear Engineering (IFIN-HH), 407 Atomistilor, Magurele-Bucharest, 077125, Romania
E-mail: Dumitru.Mihalache@nipne.ro

(Received January 14, 2008)

Abstract. We give a brief overview of recent results in the area of spatiotemporal dissipative optical solitons described by the complex cubic-quintic Ginzburg-Landau equation. We concentrate on the existence, stability and robustness of both fundamental (vorticityless) and spinning (with nonzero intrinsic vorticity) spatiotemporal dissipative solitons.

Key words: spatiotemporal optical solitons, dissipative solitons, vortex solitons, Ginzburg-Landau equation.

1. INTRODUCTION

In the last years, nonlinear localized structures in dissipative systems ("dissipative solitons") have been thoroughly investigated [1]. Specific issues, such as the existence, stability, excitation, and robustness of these localized structures in dissipative nonlinear systems have been studied in detail. In conservative (Hamiltonian) nonlinear media, the solitons (or more properly the solitary waves) are supported by a stable balance between diffraction and/or dispersion and nonlinearity, whereas, in the presence of dissipation, gain and loss must also bebalanced. In the former situation, solitons (in integrable and nonintegrable models alike) form continuous families with one or more family parameters, whereas in the latter case the condition of the balance between gain and loss results in a zero-parameter solitary-wave solution ("dissipative soliton"), having its amplitude and velocity fixed by the coefficients of the governing equations. Therefore, in dissipative nonlinear dynamical systems, the stationary soliton solutions are isolated ones; they constitutes attractors of the corresponding nonlinear dynamical system. A localized structure in a nonlinear dissipative system requires a continuous energy flow into the system, and,

in particular, into the localized structure itself, in order to preserve its shape. Therefore, the separate balance between gain and loss (or between the energy input and the energy output), seems to be more important than that between the diffraction and/or dispersion and nonlinearity. Such localized dissipative nonlinear structures occur in many areas of physics, chemistry and biology [2]. However, it is now commonly believed that the stable localized physical objects occurring in nonlinear optical media in the form of spatiotemporal dissipative optical solitons could be used to store and process information in future all-optical transmission and processing information systems [3–6].

The dissipative localized structures are modeled by nonlinear partial differential equations involving gain an loss terms in addition to the common nonlinear and dispersive/diffractive terms. These nonlinear dynamical systems allow for the formation undercertain conditions of stable dissipative solitons. One of the prototype dissipative dynamical system is that governed by the complex Ginzburg-Landau (CGL) equation, which is one of the most studied nonlinear equations in the nonlinear science [7]. It describes a vast variety of dissipative phenomena in superconductivity, superfluidity, optics and photonics, physics of lasers, Bose-Einstein condensation, liquid crystals, fluid dynamics, chemical waves, and quantum field theory. The CGL equation may be viewed as a dissipative extension of the nonlinear Schrödinger (NLS) equation; accordingly, it can describe a broad range of behaviors suggested by the NLS dynamics, ranging from chaos and pattern formation to dissipative solitons [8, 9].

The CGL equation with the cubic-quintic nonlinearity makes it possible to find stable fundamental (vorticityless) and spinning [10] localized solutions in both two-dimensional (2D) and three-dimensional (3D) geometries [11–15]. In particular, stable 2D localized states in the form of spiral waves or spiral solitons (ones with intrinsic "spin" number $S = 1$ and $S = 2$) were predicted [11]. A systematic analysis of 2D axisymmetric doughnut-shaped localized pulses with the inner phase in a form of a rotating spiral was achieved with an indication that they can be stable [11], in contrast to their NLS counterpart. Moreover, for the cubic-quintic CGL equation, three novel varieties of spiraling and nonspiralling axisymmetric solitons have been found [12]. These new localized structures are irregularly "erupting" pulses and two different types of very broad stationary ones found near a border between ordinary pulses and expanding fronts. Stable fundamental, alias spinless ($S = 0$), 3D spatiotemporal solitons [16–18], as well as double-soliton complexes, including rotating ones [19], have been found in optical models based on the cubic-quintic CGL equation. An especially challenging problem is the stability of 3D solitons with intrinsic vorticity (alias vortex tori, so called due to their doughnut-like shape), against both the supercritical collapse in the 3D space, caused by the self-focusing cubic nonlinearity [20], and the specific azimuthal instability of 3D spinning solitons [21]. However, stable 3D solitons with vorticity number $S = 1$ were found in conservative models that, to arrest the collapse, rely on competing nonlinearities, such as cubic-quintic [21] or quadratic-cubic nonlinearities [22].

Recently we have found what ingredients of the CGL model for dissipative systems are crucial to the stability of the spinless and spinning dissipative localized structures [14–15]. We have demonstrated that the diffusivity in the transverse plane is the key ingredient necessary for the stability of the spinning solitons against splitting into a set a fundamental (splinless) solitons (azimuthal instability). However, the zero-vorticity solitons may be stable in the absence of the diffusivity in the transverse plane. We have shown too that stable dissipative solitons, with zero and nonzero vorticity alike, exist at both anomalous and normal group-velocity dispersion [14]. In fact, the stability region of vortex dissipative solitons is larger in the latter case, which suggests that the solitons may be created in an expanded range of the carrier wavelength (on both sides of the zero-dispersion point). In addition, we have demonstrated that, at values of the nonlinear gain above the upper border of the existence region for stationary 3D dissipative solitons, they start either intrinsic pulsations, or permanent expansion in the temporal (longitudinal) direction, while keeping their stationary structure in the transverse plane [14]. In all these studies we have considered that the spectral filtering occur in the time domain, that is, the normalized group-velocity coefficient is a complex number, whose imaginary part account for the bandwidth-limited character of the gain. However, we have shown recently that in the absence of spectral filtering, the spatiotemporal dissipative solitons exist and are stable in certain domains of their parameter space, or in other words they exist and are stable in a dissipative system with no bandwidth-limited gain [15]. Again, the diffusivity in the transverse plane is a necessary ingredient to get stable dissipative structures even in the lack of bandwidth limited gain. These fundamental results open the way to study the interactions and collisions between both fundamental and spinning spatiotemporal solitons in dissipative systems with no bandwith-limited gain (that is, in the absence of spectral filtering).

The paper is organized as follows: After introducing the three-dimensional cubic-quintic Ginzburg-Landau model in Sec. II, in Sec. III we report results of systematic analysis of the unique features of three-dimensional fundamental and vortex dissipative solitons forming in nonlinear optical media modeled by the cubic-quintic complex Ginzburg Landau equation. The existence and stability domains of both fundamental and vortex dissipative solitons are accurately delineated. Direct numerical simulations of the evolution of perturbed dissipative solitons show full agreement with predictions based on computation of instability eigenvalues from the linearized equations for small perturbations. The paper is concluded by Section IV.

2. CUBIC-QUINTIC GINZBURG-LANDAU EQUATION

In the following we consider the 3D CGL equation with the cubic-quintic nonlinearity:

$$iU_z + \left(\frac{1}{2} - i\beta\right)\left(U_{xx} + U_{yy}\right) + \left(\frac{D}{2} - i\gamma\right)U_{tt} + \\ + \left[i\delta + (1 - i\varepsilon)|U|^2 - (\nu - i\mu)|U|^4\right]U = 0. \tag{1}$$

In the application to nonlinear optics, U is the local amplitude of the electromagnetic wave in the bulk medium, propagating along the z axis, the temporal variable being $t = T - z/V_0$, where T is time, and V_0 the group velocity of the carrier wave. Here, the coefficients which are scaled to be 1/2 and 1 account, respectively, for the diffraction in transverse plane, (x, y), and the self-focusing Kerr nonlinearity, $\beta \geq 0$ is the effective *diffusivity* in the transverse plane, the positive real constants δ, ε and μ represent, respectively, the linear loss, *nonlinear (cubic) gain*, and *nonlinear (quintic) loss*, which are basic ingredients of the cubic-quintic CGL equation in any dimension [23], $\nu \geq 0$ accounts for the self-defocusing quintic correction to the Kerr term (saturation of the optical nonlinearity), D is the group-velocity dispersion (GVD) coefficient ($D < 0$ and $D > 0$ correspond to the normal and anomalous GVD, respectively), and $\gamma > 0$ is its counterpart accounting for the *spectral filtering*, *i.e.*, the dispersion of the linear loss (it is a temporal-domain counterpart of the spatial diffusivity). We note that, in the conservative counterpart of the cubic-quintic CGL equation, *i.e.*, the NLS equation with the cubic-quintic nonlinearity, the quintic term must be self-defocusing (in the 2D and 3D settings), to suppress the collapse in the respective geometry driven by the self-focusing cubic nonlinearity [6, 21]. However, the NLS equation with the self-focusing quintic term, which appears as a natural model of Bose-Einstein condensates in the nearly one-dimensional geometry [24], gives rise to a family of stable solitons, despite the possibility of the *critical collapse* in such a setting [25]). Moreover, in Ref. [13], it was shown that the self-defocusing sign of the quintic term is not necessary for the stability of the 3D fundamental and vortex dissipative solitons, because the collapse is prevented by the action of the quintic term in the dissipative part of the equation.

We look for stationary solutions to Eq. (1) in the form of

$$U(z, x, y, t) = \psi(r, t)\exp\left(ikz + iS\theta\right), \tag{2}$$

where r and θ are the polar coordinates in plane (x, y), S is the above-mentioned integer vorticity (the fundamental solitons correspond to $S = 0$), k is a real wave number, and the complex function $\psi(r, t)$ obeys the stationary equation,

$$\left(\frac{1}{2} - i\beta\right)\left(\psi_{rr} + \frac{1}{r}\psi_r - \frac{S^2}{r^2}\psi\right) + \left(\frac{D}{2} - i\gamma\right)\psi_{tt} + \\ + \left[i\delta + (1 - i\varepsilon)|\psi|^2 - (\nu - i\mu)|\psi|^4\right]\psi = k\psi. \tag{3}$$

Localized solutions to this equation must decay exponentially at r, $|t| \to \infty$, and as r^S at $r \to 0$ (assuming $S \geq 0$). Actually, the phase fields of vortex dissipative

solitons have the form of rotating spirals in the transverse plane [11], *i.e.*, these localized patterns may also be called "spiral solitons".

To find the stationary dissipative solitons, we simulated numerically the propagation of both localized vortices and zero-vorticity solitons forward in z, within the framework of the radial version of Eq. (1), obtained by the substitution of $U(z, x, y, t) = \Psi(z, r, t)\exp(iS\theta)$, and starting with axially symmetric inputs corresponding to vorticity S,

$$\Psi(0, r, t) = Ar^S \exp\left[-\left(r^2/\rho^2 + t^2/\tau^2\right)/2\right], \tag{4}$$

with some constants A, ρ, and τ. The standard Crank-Nicholson scheme was used for the numerical integration (typically, with transverse and longitudinal stepsizes $\Delta r = \Delta t = 0.2$ and $\Delta z = 0.01$). The nonlinear finite-difference equations were solved with the help of the Picard iteration method, and the resulting linear system was then handled by means of the Gauss-Seidel iterative procedure. To achieve reliable convergence to stationary states, ten Picard and four Gauss-Seidel iterations were usually sufficient. We stress that this numerical procedure does not guarantee the stability of the so found vortex solitons, as they may be subject to instability against azimuthal perturbations [10]. The full stability was explored in a different way, see below. Finally, the wave number k of an established soliton was found as the corresponding value of the z-derivative of the phase of $\Psi(z, r, t)$, provided that it became independent on z, r and t up to five significant digits.

3. FAMILIES OF SPATIOTEMPORAL DISSIPATIVE OPTICAL SOLITONS AND THE STABILITY ANALYSIS

The results of extensive numerical simulations are presented below for $D = 1$ (anomalous GVD), a fixed coefficient of the self-defocusing quintic correction to the Kerr nonlinearity, $\nu = 0.1$, linear loss $\delta = 0.4$, and (a) *nonzero spectral filtering*, $\gamma \neq 0$, and (b) *zero spectral filtering*, $\gamma = 0.5$. The other parameters of Eq. (1), *viz.*, diffusivity coefficient β, cubic gain ε, and quintic loss μ were varied. First, we consider the case of nonzero spectral filtering ($\gamma \neq 0$). Generic results are adequately represented by existence and stability domains for both spinless and spinning solitons in the parameter plane (μ, ε) (see Fig. 1). The solitons exist between curves $\varepsilon_{upp}(\mu)$ and $\varepsilon_{low}(\mu)$, and they are *stable* in the unshaded portion of this area, which is bounded by a critical line $\varepsilon_{cr}(\mu)$, found from the linear stability analysis, see below. Below the curve $\varepsilon_{low}(\mu)$, input pulses decay to nil, whereas above the curve $\varepsilon_{upp}(\mu)$ they expand indefinitely, generating *fronts* between filled

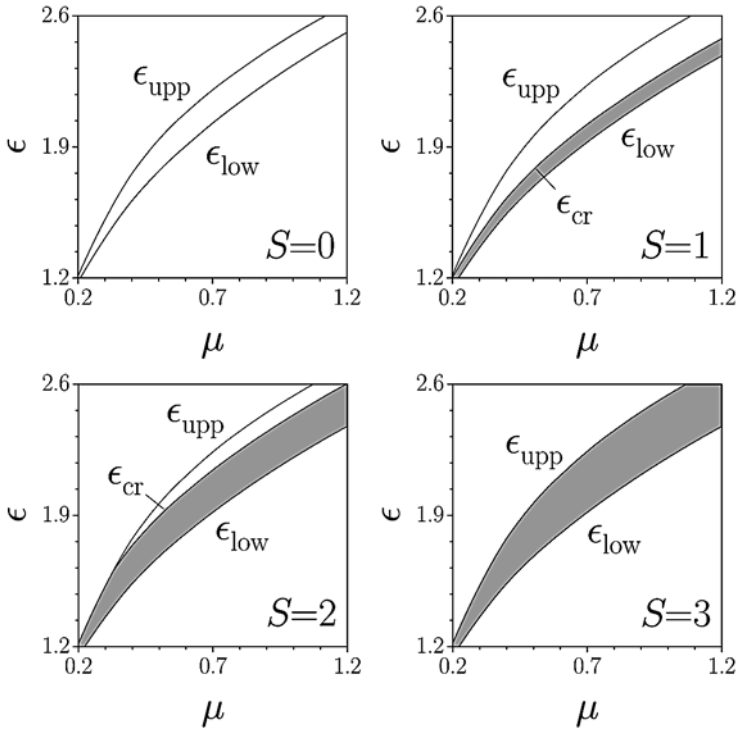

Fig. 1 – The existence and stability domains of solitons in the parameter plane (μ, ε), for spin $S = 0$, 1, 2, and 3. Other parameters are $\beta = \gamma = 1/2$, $\nu = 0.1$, and $\delta = 0.4$. In shaded regions, the solitons exist but are unstable.

and empty regions. Both the spinning and nonspinning solitons, if stable, are strong attractors, as they self-trap from a large variety of inputs.

The stability of dissipative solitons was identified through the computation of instability growth rates for eigenmodes of small perturbations. To this end, a perturbed solution to Eq. (1) was looked for as

$$\begin{aligned} U = \Big[\psi(r,t) + f(r,t)\exp\big(\lambda z + iJ\theta\big) + \\ + g^*(r,t)\exp\big(\lambda^* z - iJ\theta\big)\Big]\exp\big(ikz + iS\theta\big), \end{aligned} \tag{5}$$

where the integer J and the complex number λ are the azimuthal index and the growth rate of infinitesimal perturbations represented by eigenmodes f and g. The substitution of this expression in Eq. (1) leads to linearized equations which were solved numerically [13–15].

The predictions of the linear stability analysis were further checked in direct simulations of Eqs. (1). Initial conditions for perturbed solitons were taken as

$$U(z=0) = \psi(r,t)(1 + q\phi)\exp\big(iS\theta\big), \tag{6}$$

where q is a small perturbation amplitude, and ϕ is a random variable uniformly distributed in the interval [–0.5, 0.5]. We have checked that all the solitons that were predicted to be linearly stable are stable too against finite random perturbations. An example of self-healing of a $S = 2$ stable soliton with the initial relative perturbation amplitude of 10% is displayed in Figs. 2 and 3(a,b). On the other hand, those spinning solitons which were predicted to be unstable either decay or split into spinless solitons, if slightly perturbed. A typical example of the splitting of $S = 3$ soliton into two $S = 0$ pulses due to the azimuthal instability is shown in Figs. 3(c)–(d). The outcome agrees with the fact that the strongest instability mode for this soliton is the one with $J = 2$ [13], hence it should indeed split into two fragments.

Next, we consider the case of zero spectral filtering ($\gamma = 0$). In Fig. 4(a) and 4(b) we represent families of the 3D fundamental and vortex solitons, with $S = 0, 1, 2, 3$, by dependences of the energy,

$$E \equiv 2\pi \int_0^{\infty} rdr \int_{-\infty}^{+\infty} dt \left|\psi(r,t)\right|^2, \tag{7}$$

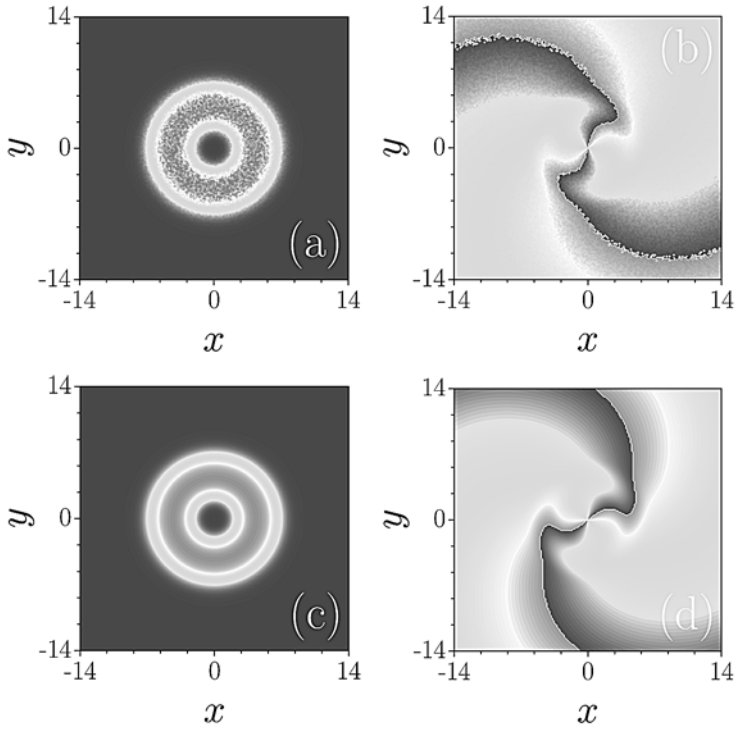

Fig. 2 – Color-scale 2D plots illustrating recovery of a perturbed stable soliton with $S = 2$, for $\mu = 1$ and $\varepsilon = 2.5$: a,b) distribution of intensity ($|U|^2$) and phase in the initial soliton perturbed by random noise: c,d) the same in the self-cleaned soliton at $z = 800$.

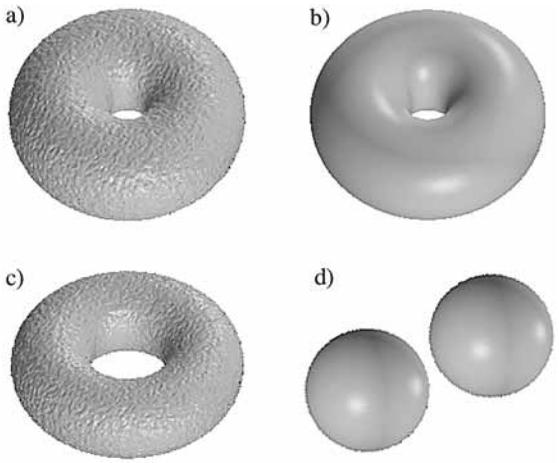

Fig. 3 – a) and b): Isosurface plots illustrating the stability of the same $S = 2$ vortex torus as in Figs. 2(a,c). Panels (a) and (b) display an initially perturbed soliton, at $z = 0$, and a self-cleaned one, at $z = 800$. c) and d): Splitting of an unstable vortex torus with $S = 3$, at $\mu = 1$ and $\varepsilon = 2.4$.

and propagation constant (wave number) k on ε, at $\beta = 0.5$ [the curve $k = k(\varepsilon)$ for $S = 3$ completely overlaps in Fig. 4(b) with its counterpart for $S = 2$]. Fig. 4 includes the results obtained by performing the linear stability analysis of 3D dissipative solitons. Here, red (or dark gray, in the black-and-white rendering) and black curves represent unstable and stable solutions, respectively. Arrows indicate stability borders.

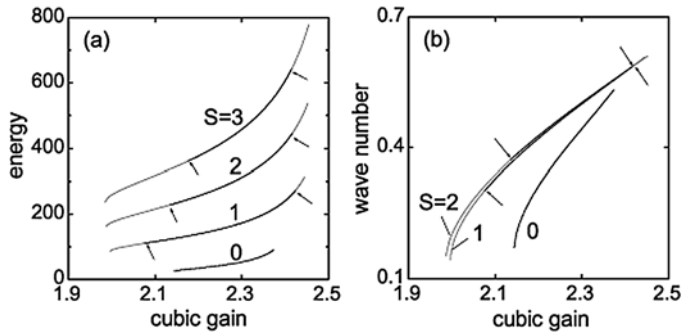

Fig. 4 – The energy (a) and wave number (b) of the fundamental and spinning dissipative solitons versus the cubic-gain parameter, ε, for $\beta = 0.5$, and $\mu = 1$.

Further, in Fig. 5 we display the existence and stability domains for the fundamental ($S = 0$) and vortex ($S = 1, 2, 3$) dissipative solitons in the plane of (μ, ε) [the quintic-loss and cubic-gain coefficients in Eq. (1)] for a nonzero diffusivity, $\beta = 0.5$. The fundamental solitons are stable in their entire existence domain, *i.e.*, between upper and lower black lines in Fig. 5(a), whereas the vortex solitons with $S = 1, 2, 3$ exist between borders $\varepsilon = \varepsilon_{upp}(\mu)$ and $\varepsilon = \varepsilon_{low}(\mu)$, being

stable in *narrower* regions, between red (or dark-gray, in the black-and-white rendering) curves in panels (b)–(d) of Fig. 5. Direct simulations demonstrate that, beneath the curves $\varepsilon = \varepsilon_{low}(\mu)$, all input pulses decay to nil, whereas above the upper borders, $\varepsilon = \varepsilon_{upp}(\mu)$, they expand indefinitely in the temporal direction, remaining localized in the spatial domain.

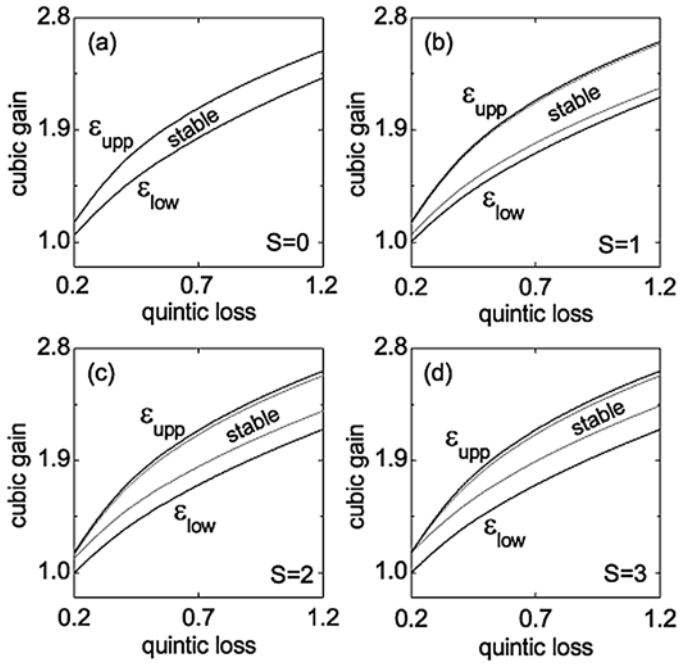

Fig. 5 – The existence and stability domains of 3D dissipative solitons, with $S = 0, 1, 2, 3$, for $\beta = 0.5$, in the plane of the quintic-loss and cubic-gain coefficients, (μ, ε).

As mentioned above, and stated in Ref. [14] for the setting with $\gamma > 0$, the transverse diffusivity, $\beta > 0$, is necessary for the stability of all vortex dissipative solitons, but not of their fundamental counterparts. This conclusion remains also true in the Ginzburg-Landau model with zero spectral filtering, $\gamma = 0$, as illustrated by Fig. 6. In particular, if $\beta = 0$, the perturbation eigenmode with azimuthal index $J = 2$ [see Eq. (5)] destabilizes the family of the $S = 1$ vortex dissipative solitons in the *entire* region of their existence, see Fig. 6(c).

In the case when the diffusivity is present ($\beta = 0.5$), typical results of the linear stability analysis for the 3D vortex dissipative solitons are displayed in Fig. 7, where, fixing $\mu = 1$, we display the largest instability growth rate versus nonlinear gain ε (stability regions revealed by this figure are included in the stability diagrams

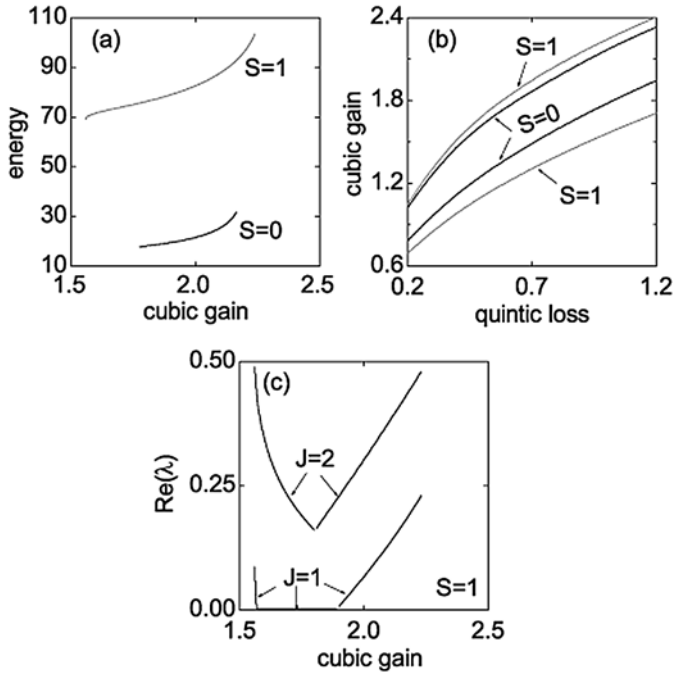

Fig. 6 – (a) The energy of fundamental ($S = 0$) and vortex ($S = 1$) 3D dissipative solitons versus the nonlinear-gain parameter ε, for *zero diffusivity*, $\beta = 0$. (b) The existence and stability domains for these solutions. (c) The largest instability growth rate versus ε for the vortex solitons with $S = 1$.

in Fig. 4). Note that actual borders of the stability regions for the vortex solitons with vorticity S are determined by the perturbation eigenmodes with $J = S$. Thus, it is plausible that smaller stability regions can be found, for $\beta > 0$ (and $\gamma \geq 0$) also for spinning solitons with vorticities $S > 3$ (see Fig. 7).

The stable 3D dissipative solitons are *strong attractors*: direct simulations demonstrate that an arbitrary initial waveform with intrinsic vorticity S readily converges to the respective spinning soliton. Accordingly, the dissipative solitons which are predicted to be stable by the linear analysis, turn out to be robust against the addition of non-small initial perturbations, as shown in Fig. 8 for the vortex soliton with $S = 3$, the initial perturbation amplitude taken at the level of 10%. The numerical simulations were run on a three-dimensional grid of size $[-20, 20] \times [-20, 20] \times [-14, 14]$. Thus we have shown the first ever example of stable higher-order vortex tori (with $S > 1$), and also the first example of stable vortex solitons in a 3D dissipative medium. These results, obtained in the paradigmatic CGL model, suggest that similar stable localized objects with intrinsic vorticity may also be found in more complex 3D dissipative models.

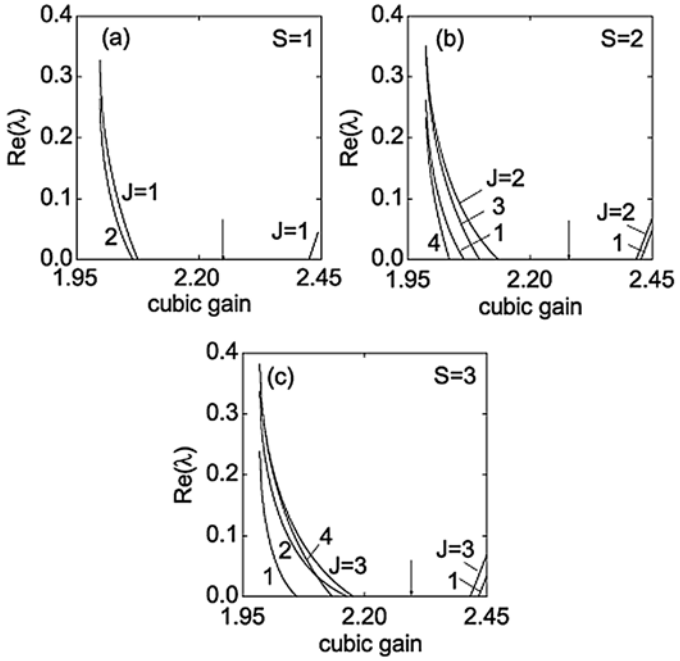

Fig. 7 – The largest instability growth rate versus ε for vortex 3D dissipative solitons: a) $S = 1$, b) $S = 2$, c) $S = 3$. Other parameters are $\mu = 1$, $\beta = 0.5$ (and $\gamma = 0$). The arrows indicate centers of the stability intervals.

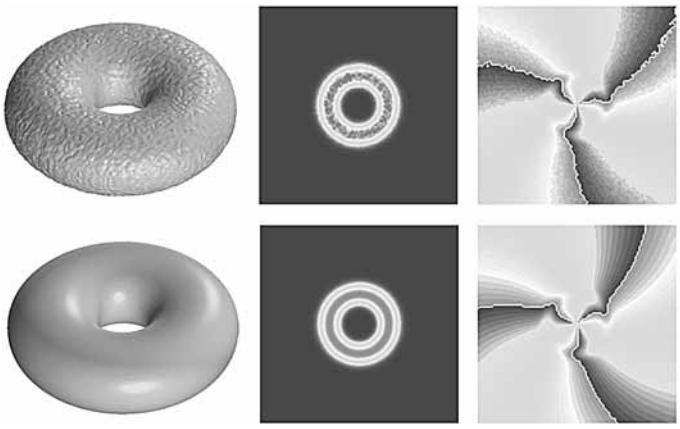

Fig. 8 – The recovery of a perturbed 3D vortex soliton with $S = 3$, for $\mu = 1$, $\beta = 0.5$ and $\varepsilon = 2.3$. Upper row: the intensity ($|U|^2$) and phase of the initial soliton perturbed by random noise. Lower row: The same in the self-cleaned soliton at $z = 800$.

4. CONCLUSIONS

We have briefly reviewed the recent analysis of conditions for the existence and stability of three-dimensional dissipative solitons with intrinsic vorticity S in the complex Ginzburg-Landau equation with the cubic-quintic nonlinearity, in both dissipative and conservative parts of the equation. Essential conclusions are that nonzero diffusivity in the transverse plane ($\beta > 0$) is a necessary stability condition for all vortex dissipative solitons, with $S \geq 1$, but not for the fundamental (vorticityless) solitons ($S = 0$). At $ta \geq 0$, the fundamental dissipative solitons are stable in their entire existence area, while the dissipative vortex solitons are stable only for nonzero diffusivity ($\beta > 0$) in a part of their existence range. In large-aspect ratio lasers, condition $\beta > 0$ corresponds to negative detuning. On the other hand, the presence of the spectral filtering (that is, the temporal-domain diffusivity, which, in the laser-cavity models accounts for the finite gain bandwidth) is not necessary for the stability of any type of dissipative solitons, which opens the way to study collisions between stable three-dimensional spatiotemporal dissipative solitons moving in the longitudinal direction. The simplest and the more tractable physical setting is when the three-dimensional solitons form a coaxial configuration; therefore on-axis collisions between solitons with both equal and diferent vorticities can be investigated.

Acknowledgements. Part of the research work overviewed in this paper has been carried out in collaboration with Lucian-Cornel Crasovan, Yaroslav V. Kartashov, Hervé Leblond, Falk Lederer, Boris A. Malomed, and Lluis Torner. We are deeply indebted to all of them.

REFERENCES

1. N. Akhmediev, A. Ankiewicz (Eds.), *Dissipative Solitons*, Lect. Notes Phys., **661**, Springer, Berlin, 2005.
2. G. Nicolis, I. Prigogine, *Self-organization in nonequilibrium systems*, John Wiley and Sons, New York, 1977.
3. Yu. S. Kivshar, G. P. Agrawal, *Optical solitons: From fibers to photonic crystals*, Academic Press, San Diego, 2003.
4. N. N. Akhmediev, A. Ankiewicz, *Solitons: Nonlinear Pulses and Beams*,Chapman and Hall, London, 1997.
5. G. I. Stegeman, D. N. Christodoulides, M. Segev, IEEE J. Select. Top. Quant. Electron., **6**, 1419 (2000).
6. B. A. Malomed, D. Mihalache, F. Wise, L. Torner, J. Opt. B: Quantum Semiclassical Opt., **7**, R53 (2005).
7. I. S. Aranson, L. Kramer, Rev. Mod. Phys., **74**, 99 (2002); P. Mandel, M. Tlidi, J. Opt. B: Quantum Semiclass. Opt., **6**, R60 (2004); B. A. Malomed, in *Encyclopedia of Nonlinear Science*, p. 157. A. Scott (Ed.), Routledge, New York, 2005.
8. N. N. Rosanov, *Spatial Hysteresis and Optical Patterns*, Springer, Berlin, 2002.

9. S. Barland, J. R. Tredicce, M. Brambilla, L. A. Lugiato, S. Balle, M. Giudici, T. Maggipinto, L. Spinelli, G. Tissoni, T. Knodl, M. Miller, R. Jager, Nature (London), **419**, 699 (2002); Z. Bakonyi, D. Michaelis, U. Peschel, G. Onishchukov, F. Lederer, J. Opt. Soc. Am. B, **19**, 487 (2002); E. A. Ultanir, G. I. Stegeman, D. Michaelis, C. H. Lange, F. Lederer, Phys. Rev. Lett., **90**, 253903 (2003).
10. W. J. Firth, D. V. Skryabin, Phys. Rev. Lett., **79**, 2450 (1997).
11. L.-C. Crasovan, B. A. Malomed, D. Mihalache, Phys. Rev. E, **63**, 016605 (2001).
12. L.-C. Crasovan, B. A. Malomed, D. Mihalache, Phys. Lett. A, **289**, 59 (2001).
13. D. Mihalache, D. Mazilu, F. Lederer, Y. V. Kartashov, L.-C. Crasovan, L. Torner, B. A. Malomed, Phys. Rev. Lett., **97**, 073904 (2006).
14. D. Mihalache, D. Mazilu, F. Lederer, H. Leblond, B. A. Malomed, Phys. Rev. A, **75**, 033811 (2007).
15. D. Mihalache, D. Mazilu, F. Lederer, H. Leblond, B. A. Malomed, Phys. Rev. A, **76**, 045803 (2007).
16. P. Grelu, J. M. Soto-Crespo, N. Akhmediev, Opt. Express, **13**, 9352 (2005).
17. J. M. Soto-Crespo, P. Grelu, N. Akhmediev, Opt. Express, **14**, 4013 (2006).
18. V. Skarka, N. B. Aleksić, Phys. Rev. Lett., **96**, 013903 (2006).
19. J. M. Soto-Crespo, N. Akhmediev, P. Grelu, Phys. Rev. E, **74**, 046612 (2006); N. Akhmediev, J. M. Soto-Crespo, P. Grelu, Chaos, **17**, 037112 (2007).
20. L. Bergé, Phys. Rep., **303**, 260 (1998).
21. D. Mihalache, D. Mazilu, L.-C. Crasovan, I. Towers, A. V. Buryak, B. A. Malomed, L. Torner, J. P. Torres, F. Lederer, Phys. Rev. Lett., **88**, 073902 (2002).
22. D. Mihalache, D. Mazilu, L.-C. Crasovan, I. Towers, B. A. Malomed, A. V. Buryak, L. Torner, F. Lederer, Phys. Rev. E, **66**, 016613 (2002).
23. V. I. Petviashvili, A. M. Sergeev, Dokl. Akad. Nauk SSSR, **276**, 1380 (1984) [Sov. Phys. Dokl., **29**, 493 (1984)].
24. A. E. Muryshev, G. V. Shlyapnikov, W. Ertmer, K. Sengstock, M. Lewenstein, Phys. Rev. Lett., **89**, 110401 (2002); L. Salasnich, A. Parola, L. Reatto, Phys. Rev. A, **65**, 043614 (2002).
25. D. E. Pelinovsky, Y. S. Kivshar, V. V. Afanasjev, Physica D, **116**, 121 (1998); L. Khaykovich, B. A. Malomed, Phys. Rev. A, **74**, 023607 (2006).